UDK 621.771:669.017.3

Microstructural Behaviour of Tempering Steels during Precision Forging and Quenching from Hot-forming Temperatures

F. Nürnberger, O. Grydin, Z. Yu, M. Schaper

Faculty of Mechanical Engineering, Institute of Materials Science,
Leibniz University Hanover, An der Universität 2, 30823 Garbsen, Germany,
nuernberger@iw.uni-hannover.de

To design a precision forging or twin-roll casting process combined with heat treating from the hot-forming temperature, flow curves for a selection of hardening and tempering steels were recorded using a deformation dilatometer. In addition to this, continuous cooling transformation diagrams were generated for the 42CrMo4 hardening and tempering steel. These diagrams take into account the influence of deformation on the transformation behaviour during quenching from a temperature of 850 °C. The results of the investigations show an increase in the flow stresses with decreasing temperatures and the deformation's minor influence on the resulting material's hardness and microstructural constituents.

Keywords: TEMPERING STEEL, QUENCHING FROM HOT-FORMING TEMPERATURE, FLOW CURVES, CCT

1. Introduction

The controlled heat treatment of hardening and tempering steels using the hot forming temperature of metal forming processes such as precision-forging, deep drawing or twin-roll casting enables significant savings of resources in comparison to conventional methods. On the one hand, a smaller amount of material is required during flashless precision forging since the usual proportion of flash of approx. 30% is eliminated. On the other hand, the forgings already have their final near-net shapes [1] so that the available hot-forming heat can be employed to heat treat the material [2]. Twin-roll casting allows high energy and material savings due to the highly reduced manufacturing chain, since most of the conventionally necessary steps of hot rolling can economized. Among the materials specially developed for heat treating from the hot-forming heat comprise, for instance, the AFP-steels with which a controlled transformation is carried out into the pearlite stage. Typical AFP-steels are the alloys 38MnVS6 and 46MnVS3. The essential mechanism for increasing hardness values during the controlled cooling is the selective solid-solution and precipitation hardening for these steels [3]. The ultimate strengths of conventional hardening and tempering steels, such as 42CrMo4, are, however, currently not obtainable using these materials [4]. Relatively soft martensitic steels, such as 10MnB6 or 5CrB4 alloys, enable quenching to simultaneously produce a martensitic microstructure and reduced susceptibility to cracking [5]. Also, air-hardening steels such as 21CrMnCu8-6 and 40SiMnCrMo7-6-6-4 or LH800 materials are suitable for obtaining a martensitic microstructure during cooling in still air. Additional steels are employed in the automotive industry, particularly for crash-relevant parts, such as 22MnB5 sheet material alloyed with boron for manufacturing extremely high strength body elements by means of press-hardening using heated, closed dies [6]. Conventional hardening and tempering steels are not generally employed in these processes but they offer the possibility, particularly with controlled cooling using locally variable cooling rates, of manufacturing high strength, bulk-formed components possessing various requirements matched to functional surfaces. This is possible by means of, for example, spatially varied and temporally controlled cooling based on water-air spraying [7].

During the controlled cooling from the hot-forming temperature with the aim of obtaining spatially different microstructures, it is essential to take account of the microstructure's transformation behaviour which is influenced by the forming and the austenitising temperatures. Deformation time-temperature-transformation diagrams (Deformation TTT diagrams) and deformation continuous cooling

transformation diagrams (CCT diagrams) can map these circumstances [8]. Thus, it was possible for *Weise* to represent the transformation behaviour with respect to hot rolling a 42CrMo4 hardening and tempering steel and austenitising temperatures of 900 °C [9]. Moreover, investigations of the microstructure's transformation kinetics were carried out at austenitising temperatures of 1200 °C and true strains of up to 0.6 for isothermal [10] and continuous cooling [11]. Especially during isothermally controlled temperatures, changes in the transformation intervals can be established whereas the microstructures mainly change their distinctive features during a continuous transformation.

2. Objectives

To design metal forming processes in combination with the hardening and tempering using the hot-forming temperature, flow curves are required for the process simulation. These curves are recorded by means of a deformation dilatometer for a selection of heat treatable steels by which cylindrical specimens are compressed to true strains of up to 0.6. Furthermore, deformation continuous cooling transformation diagrams are required which take into account the influence of a deformation on the transformation behaviour during quenching. In addition to the deformation CCT diagrams for austenitising temperatures of 900 °C [9] and 1200 °C [11], which are already available in the literature, supplementary diagrams are required for the 42CrMo4 heat treatable steel at other austenitising and deformation temperatures. Within the scope of this work, the transformation behaviour is characterised at additional austenitising temperatures from 850 °C. The diagrams are generated by employing linear cooling rates so that it is possible to subsequently compute the isothermal transformation kinetics or, as the case may be, the isothermal deformation TTT diagrams based on an approach according to *Rios* [12, 13]. The context for this is that isothermal diagrams, which require relatively less effort to generate, can be employed for the numerical design procedures to predict microstructures for arbitrary cooling profiles [14].

3. Materials and methods

3.1. Chemical composition of the investigated materials

A selection of heat treatable steels, 34CrMo4, 42CrMo4, 50CrMo4, 51CrV4 and 34CrNiMo6, were used for the experimental investigations of the continuous transformation behaviour and to record the flow curves. The chemical composition in weight % determined by means of Glow Discharge Optical Spectroscopy GDOS is given in **Table 1**. The measurements were performed on polished specimens using a GDA 550 device made by the company Spectruma. The alloys' compositions differ, particularly in their carbon contents, which is decisive for their strength. Moreover, the 34CrNiMo6 alloy is distinguished by its high nickel and chromium content for its ability to be fully quenched and tempered as large forgings or thick-walled parts.

Table 1. Chemical compositions of the used alloying elements in weight %

alloy	C	Si	Mn	P	S	Cr	Cu	Mo	Ni	Al	Nb
34CrMo4	0.325	0.289	0.577	0.007	0.003	0.945	0.286	0.132	0.098	0.025	0.019
42CrMo4	0.410	0.336	0.701	0.011	0.025	0.998	0.380	0.171	0.191	0.029	0.019
50CrMo4	0.491	0.212	0.647	0.005	0.004	1.039	0.219	0.133	0.092	0.024	0.020
51CrV4	0.467	0.223	0.845	0.006	0.017	1.015	0.223	0.013	0.083	0.018	0.063
34CrNiMo6	0.326	0.263	0.588	0.001	0.004	1.433	0.260	0.126	1.469	0.023	0.020

3.2. Dilatometric measurements

The microstructural transformations produced during cooling from the hot-forming temperature are influenced by the austenitising temperatures and the deformation strain. To simulate the metal forming processes, material samples of the investigated 42CrMo4 alloy (5 mm diameter, 10 mm long) were inductively heated to an austenitising temperature of 850 °C within 30 s. Following isothermal soaking for 600 s, samples were deformed to true strains of 0.16 or 0.35, as the case may be, at a deformation rate of 1 s^{-1}. Following this, the samples were linearly cooled using cooling rates in the region of 50 K s^{-1} to 0.02 K s^{-1} (see **Figure 1**).

For reference purposes, a diagram was constructed without deformation. The measurements were carried out using a deformation dilatometer DIL 805A/D, made by the company BÄHR-Thermoanalyse GmbH, (see **Table 2**) in collaboration with the Częstochowa University of Technology, Poland. The investigations were carried out according to the Polish standard PN-68/H-04500, which essentially corresponds to the German "Stahl-Eisen-Prüfblättern" SEP 1680 or SEP 1681, as the case may be. The start and finish of the respective microstructural transformations were determined from the measured length changes of the dilatometer's time-profile curves as well as from the metallographic

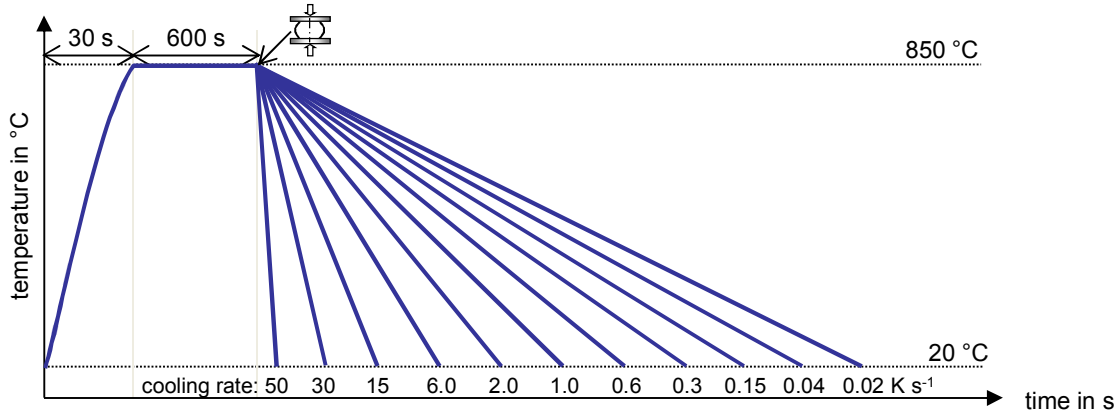

Figure 1. Schematic of the time-temperature controlled linear cooling profiles for generating the deformation CCT diagrams

Table 2. Technical of the quench and deformation dilatometer device DIL 805 A/D, made by the company Thermoanalyse Bähr GmbH

Device's properties	Characteristics of the deformation dilatometer
Temperature range	20 °C to 1500 °C
Heating method	inductive
Specimen material	electrically conducting solid
Atmosphere	shielding gas, vacuum, air
Resolution Δl and °C	0.05 µm; 0.05 °C
Specimen geometry	Solid specimens (5 mm diameter, 10 mm long)
Heating and cooling rate	max. 100 K s^{-1}
Applied deforming force	max. 25 kN
Ram velocity	0.01 mm s^{-1} to 125 mm s^{-1}
Strain rate	0.1 s^{-1} to 12.5 s^{-1}
True strain	0.05 to 1.2

analyses and hardness measurements. For reasons of readability, no hardness values are given in the constructed deformation CCT diagrams. The curves in the diagrams for the start and finish of the transformations were drawn by hand. Based on the selected minimum cooling rate of 0.02 K s^{-1}, only a few data points exist for the ferrite or, as the case may be, the pearlite regions so that the depicted curves' trajectories for longer periods of time represent an estimate. Lower cooling rates are not technically relevant for above mentioned metal forming processes with integrated heat-treatment since this cooling rate already corresponds to a cooling period of more than 11 h to reach room temperature from the hot forming temperature.

3.3. Metallographic specimen analysis

To quantitatively measure the microstructural constituents following the dilatometry tests, the specimens were first embedded at room temperature and longitudinal segments, along the specimen's axis of rotation, were subsequently ground and polished. The preparation was carried out using a heat avoiding process by wet grinding with increasing paper grades. The locations of the micrographic images and the subsequent hardness measurements were 1/3 of the specimen's radius and 1/3 of its length [15]. The specimens were polished to 1 µm and etched using 2 % nitric acid (HNO_3) in order to contrast the individual constituents. By means of an Axioplan reflecting light microscope made by the company Zeiss and a digital camera, digital images were produced at various magnifications. The various microstructures occurring in the different materials are generally differentiated by means of their characteristic size, form, alignment and colour. Moreover, a microstructure can be identified by using a low-load or micro hardness tester since the various microstructures differ due to their structural hardness values. For measuring the phase fractions of the individual microstructural constituents, the frequency distribution, for example, of the micrographic images' brightness (histogram) can be employed. The software analySIS doc 5.0 was employed for differentially determining the microstructural fractions in the HIS-space using the colour tones, saturation and intensity. For

this purpose, the digital image data was initially prepared in which the pixel errors were removed by using median filters. In addition to this, the contrast was boosted using a DCE (differential contrast enhancement) filter. With respect to the individual microstructural fractions, it can be assumed that the measuring error is just a few percentage points.

3.4. Hardness measurements

To characterize the hardness of the dilatometer specimens' microstructure, tests were carried out according to DIN EN ISO 6507-1 using either an Instron-Wolpert-Testor 930/250 or a Duramin 20, fully automated micro hardness tester made by the company Struers. The functionality of the employed hardness testing device was controlled prior to starting the test by means of a calibrated hardness-reference piece. The relative error was less than 0.2 %. Four hardness measurements HV10 were performed on each of the dilatometer specimens in their unetched condition. The respective mean values were calculated and, where appropriate, supplemented by low-load hardness tests HV0.1 in the etched condition to identify the structural phase.

3.5. Flow curves

The flow curves required for numerically representing the process were determined from steel specimens (5 mm diameter, 10 mm long) of the 5 alloys investigated here for an austenitising and a soaking temperature of 1200 °C. For this purpose, the specimens were inductively heated within 30 s to 1200 °C. Following isothermal soaking for 600 s, samples were plastic deformed to true strains of 0.6 using a strain rate of 1 s^{-1}. In addition to this, flow curves for the 42CrMo4 hardening and tempering steel were determined for austenitising and forming temperatures of 1050 °C and 850 °C. The logarithmic or true strain φ and the flow stress k_f corresponding to equation 1 and equation 2, respectively, were computed from the measured force-displacement curve. Plotting k_f against φ gives the corresponding flow curve where L_0 signifies the specimen's initial length, L_1 the current length and r_0 the specimen's initial radius. F is the measured applied force. For each combination of material and forming temperature, five flow curve profiles each were evaluated and using a regression analysis, a mean flow curve was computed by employing Software Datafit 8.0.32 developed by the company Oakdale Engineering. equation 3 was applied as the modelling approach according to a flow curve model of *Hensel* and *Spittel* [16], which takes into account the true strain and the forming temperature.

$$\varphi = \ln\left(\frac{L_1}{L_0}\right) \qquad \text{(Eq. 1)}$$

$$k_f = F\left(\frac{L_1}{\pi \cdot r_0^2 \cdot L_0}\right) \qquad \text{(Eq. 2)}$$

$$k_f = a_0 \cdot \varphi^{a_1} \cdot \exp(a_2 \cdot \varphi) \cdot \exp(-a_3 \cdot T) \qquad \text{(Eq. 3)}$$

Since only flow curves at the forming temperature of 1200 °C were recorded for the 34CrMo4, 50CrMo4, 51CrV4 and 34CrNiMo6 hardening and tempering steels, a regression analysis was performed by assuming that $a_3 = 0$ is valid in this case.

4. Results and discussion

4.1. Flow curves

The measured flow curves modelled according to equation 3 are depicted in **Figure 2**. The curves' trajectories for the five alloys exhibit very similar profiles at a forming temperature of 1200 °C. Here, the flow stress initially rises almost linearly and, following a flattening, reaches a maximum flow stress of approx. 55 MPa to 65 MPa at true strains of about 0.2 to 0.3. Subsequent to this, the flow stress falls until the maximum true strain of 0.6 is reached at about 5 MPa to 10 MPa, respectively. **Table 3** contains the parameters determined according to equation 3 of the approach by *Hensel* and *Spittel* by specifying the coefficient of multiple determination R^2 and the maximum error *ME* as well as the respective austenitising temperature T_A. For example, the 42CrMo4 hardening and tempering steel shows that the maximum flow stresses significantly increase from 67 MPa and 99 MPa to 190 MPa for decreasing forming temperatures from 1200 °C and 1050 °C to 850 °C, respectively. This corresponds to almost a tripling of the maximum flow stress. In comparison to the models according to *Hensel* and *Spittel* [16], very good agreement within the considered interval is reached for forming temperatures of 1200 °C and 1050 °C. However, the flow curve's profile measured here for the forming temperature of 850 °C lies approx. 30 MPa above the values specified by the model. Moreover, the drop in stress following its maximum value at true strains of approx. 0.2 to 0.3 remains neglected using the considered model. Coefficient of multiple determination R^2 for the investigated alloy 34CrMo4 is comparatively low since scattering of the five as an input used flow curves, though the approximation itself can be assumed highly accurate.

4.2. Evaluation of the microstructure

The CCT diagram for the steel 42CrMo4 (see **Figure 3**, top) exhibits ferritic, pearlitic, bainitic and martensitic constituents. The measured upper critical cooling rate is 15 K s^{-1}. Bainite is formed at cooling rates of between 6 K s^{-1} and 0.3 K s^{-1}. Ferrite and pearlite can be established at cooling rates from 1 K s^{-1} and less (see **Table 4**). Between the regions of martensite and bainite formation as well as between bainite and pearlite formation there is a temperature interval which is free of transformations.

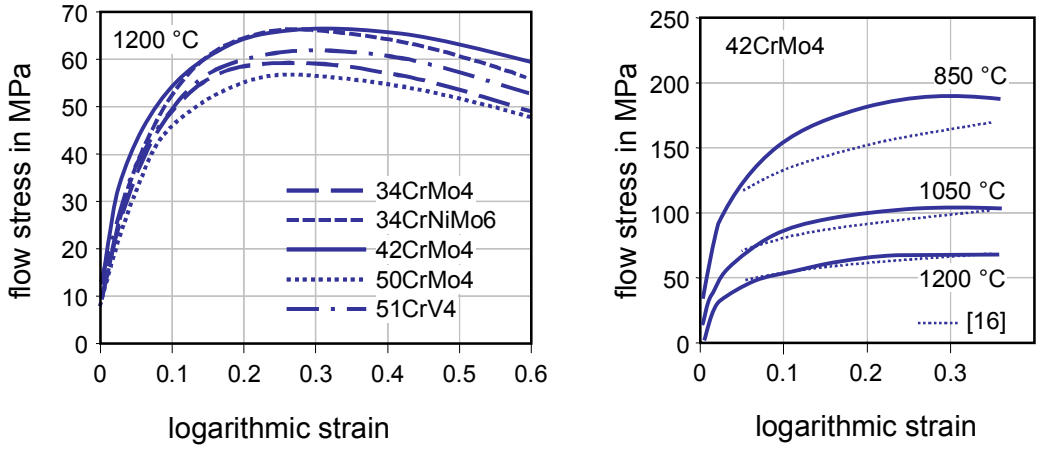

Figure 2. Flow curves according to equation 3 determined by means of a regression analysis for various materials and forming temperatures; deformation rate 1 s^{-1}. As a comparison, the computed flow curves according to the approaches of *Hensel* and *Spittel* [16] are depicted in the right hand figure

Table 3. Regression parameters for the flow curves according to equation 3 each determined from the regression analysis of 5 measurements; R^2: coefficient of multiple determination; *ME*: maximum error in %; T_A: austenitising temperature

T_A	1200 °C	850 °C to 1200 °C	1200 °C	1200 °C	1200 °C
alloy	34CrMo4	42CrMo4	50CrMo4	51CrV4	34CrNiMo6
a_0	196	6000	175	180	233
a_1	0.526	0.422	0.508	0.488	0.570
a_2	-1.875	-1.335	-1.735	-1.613	-1.892
a_3	0	0.003	0	0	0
R^2	> 0.64	> 0.91	> 0.93	> 0.91	> 0.93
ME	12.5	9.1	5.8	6.1	4.8

Table 4. Metallographically determined microstructural constituents as well as hardness values of 42CrMo4 heat treatable steel specimens for various linear cooling rates in K s^{-1} and true strains φ at austenitising and forming temperatures of 850 °C

φ	K s^{-1}	50	30	15	6	2	1	0.60	0.30	0.15	0.04	0.02
0	F	-	-	-	-	-	2	4	6	15	12	15
	P	-	-	-	-	-	*)	3	50	85	88	85
	B	-	-	-	4	18	42	58	27	-	-	-
	M	100	100	100	96	82	56	35	17	-	-	-
	HV	723	-	705	673	598	470	408	340	242	219	219
0.16	F	-	-	-	-	-	3	3	4	5	12	15
	P	-	-	-	-	-	*)	7	23	58	88	85
	B	-	-	-	**)	12	45	59	40	37	-	-
	M	100	100	100	100	88	52	31	33	**)	-	-
	HV	719	732	724	696	595	450	407	345	317	237	234
0.35	F	-	-	-	-	**)	**)	2	1	8	12	11
	P	-	-	-	-	-	-	1	1	71	88	89
	B	-	-	-	3	17	44	68	90	20	-	-
	M	100	100	100	97	81	56	29	8	1	-	-
	HV	730	725	721	701	585	470	448	361	297	240	221

F: ferrite, P: pearlite, B: bainite, M: martensite, HV: Vickers hardness in HV10
*) Traces in the segregations, **) Traces in the microstructure

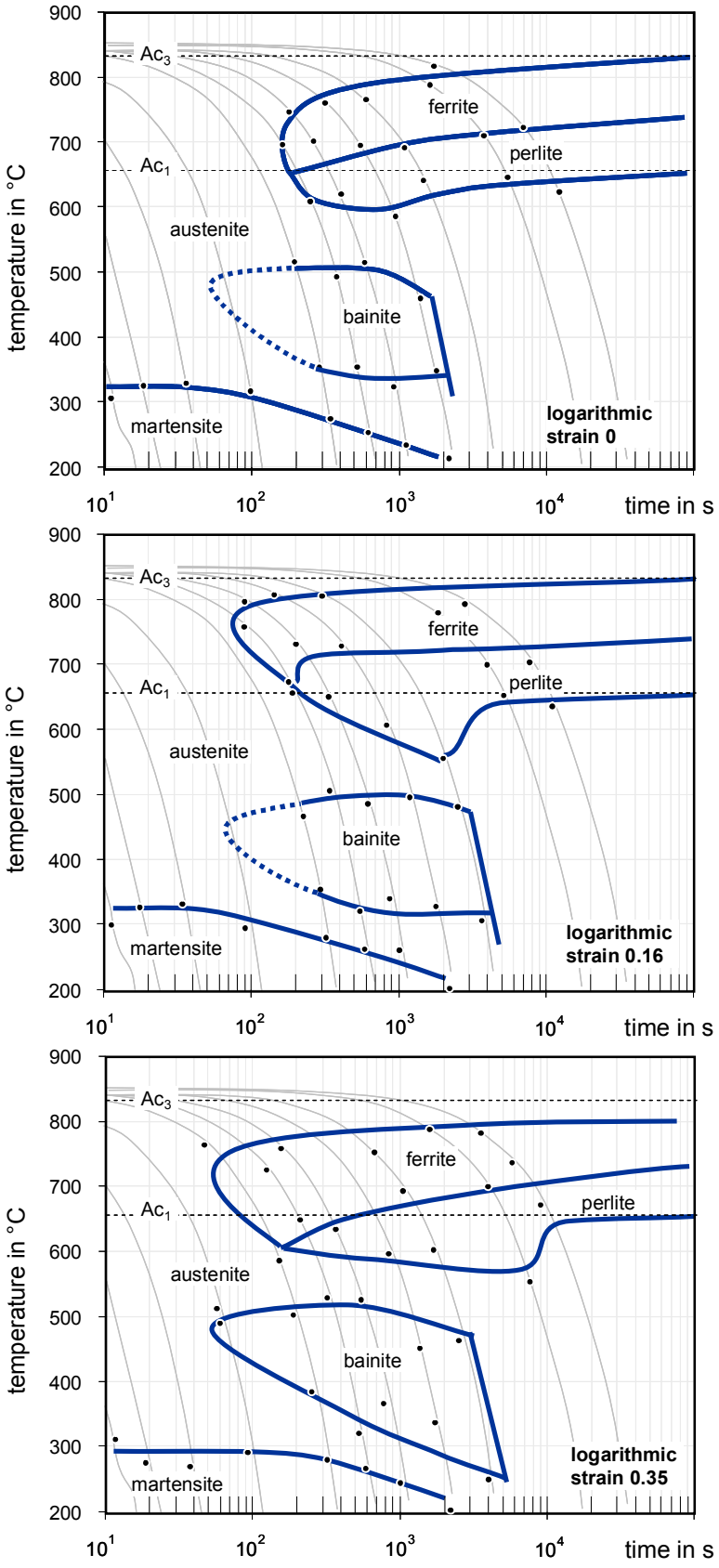

Figure 3. Deformation CCT diagrams for the materials 42CrMo4 for logarithmic strains of 0 (top), 0.16 (centre) and 0.35 (bottom), austenitising temperature 850 °C

A deformation of 16 % (see **Figure 3**, centre) produces a slowly accelerated ferrite transformation together with bainite, which is also formed at lower cooling rates. The pearlite stage's temperature interval is somewhat broadened. On increasing the deformation further to 35 %, the ferrite's transformation temperature interval is also augmented (see **Figure 3)** and the start of the pearlite formation is shifted to slower cooling rates. The martensite's start temperature drops with increasing deformation to below 300 °C. A comparison of the microstructural constituents formed at different deformations exhibits reduced fractions of pearlite at a cooling rate of 0.3 K s^{-1} (see **Table 4** and **Figure 4**).

The deformation tends to lead to a slight increase in hardness values. As a consequence of the broadening of the bainite field with increasing deformation, an additional increase in hardness results at lower cooling rates due to the elevated bainite content.

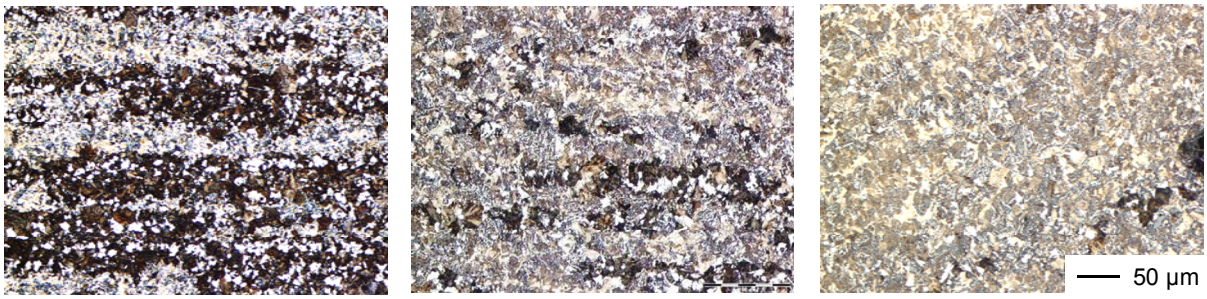

Figure 4. 42CrMo4 hardening and tempering steel's microstructure cooled at 0.3 K s^{-1} for logarithmic strains varied from 0, 0.16 and 0.35 (2 % HNO_3)

5. Conclusions

The work carried out here produced the following results:

The flow curves for the five hardening and tempering steels considered here exhibit comparable profiles possessing a maximum true strain at approx. 0.2 or 0.3 and maximum flow stresses from 55 MPa to 65 MPa at deformation temperatures of 1200 °C. In contrast to the data according to [16], a drop in the flow stress can be discerned after attaining a maximum value.

i) Flow curves for the 42CrMo4 hardening and tempering steel show a marked rise in the flow stresses by a factor of approx. 2.9 with falling deformation temperatures within the temperature interval from 1200 °C to 850 °C.

ii) For the hardening and tempering steel, a deformation at the austenitising and deformation temperatures of 850 °C exerts only a small influence on the material's hardness value which exists following cooling. In contrast to this, the hardness value is substantially influenced by the selected cooling rate.

iii) The metallographic analyses show that the bainite field, in particular, broadens to later times as a consequence of the deformation and larger fractions of bainite are formed. Furthermore, a drop in the martensite start temperature is established.

Future work is planned to determine the transformation behaviour for austenitising and deformation temperatures from 1050 °C by using the 42CrMo4 hardening and tempering steel as an example. In doing this, the investigations in [11] will be augmented and the complete deformation time-temperature-transformation behaviour for this material would be recorded for the temperature interval from 850 °C to 1200 °C.

Acknowledgements

The authors would like to thank the German Research Foundation (DFG) for their financial support of the work carried out within the scope of the Collaborative Research Centre 489, sub project A3 as well as Ms. M. Reiter and Mr. K. Oelker for supporting the materials' and metallographic analyses. Special thanks go Dr. eng. B. Koczurkiewicz and Prof. Dr. hab. inż. A. Milenin regarding the dilatometric investigations at the Częstochowa University of Technology, Poland.

References

1. Behrens, B.-A.; D. Odening, S. Müller, M. Lücke: *Process Design and Tooling Configuration for Precision Forging of High Performance Components*. Steel Research International 80 (2009), 12, pp. 869-877

2. Gretzki, T.; Krause, C.; Frolov, I.; Nicolaus, M.; Hassel, Th.; Bach, Fr.-W.; Kästner, M.; Abo-Namous, O.; Reithmeier, E.: *Manufacturing surface hardened components of 42CrMo4 by water-air spray cooling*. Steel Research international 80 (2009), 12, pp. 906-915

3. Bleck, W.; Keul, C.; Zeislmair, B.: *Entwicklung eines höherfesten mikrolegierten ausscheidungshärtenden ferritisch/perlitischen Schmiedestahls AFP-M*. Schmiede-Journal, 03/2010, pp. 42-44

4. Muckelbauer, M.; Arndt, J.: *Schmiedeteile behaupten sich erfolgreich im Technologiewettbewerb*. Schmiede-Journal (2008), 3, pp. 36-38

5. Wegner, K.-W.: *Werkstoffentwicklung für Schmiedeteile im Automobilbau*. ATZ Automobiltechnische Zeitschrift 100 (1998), 12, pp. 918-927

6. Lechler, J.: *Beschreibung und Modellierung des Werkstoffverhaltens von presshärtbaren Bor-Manganstählen*. Diss., Friedrich-Alexander-Universität Erlangen-Nürnberger, 2008

7. Krause, C.; Hassel, T.; Frolov, I.; Gretzki, T.; Kästner, M.; Seewig, J.; Bormann, D.; Bach, Fr.-W.: *Randschichtvergüten von Zahnwellen mittels Wasser-Luft-Sprühkühlung*. HTM 63 (2008), 1, pp. 22-26

8. Kaspar, R.; Lotter, U.; Biegus, C.: *The influence of thermomechanical treatment on the transformation behaviour of steels*. Steel Research 65 (1994), 6, pp. 242-247

9. Weise, A.: *Entwicklung von Gefüge und Eigenspannungen bei der thermomechanischen Behandlung des Stahls 42CrMo4*. Diss., TU Chemnitz, 1998

10. Nürnberger, F.; Grydin, O.; Schaper, M.; Bach, Fr.-W.; Evertz, T.; Kluge, U.: *Isothermal Microstructural Transformations of the Heat-treatable Steel 42CrMo4 during Heat-treatment following Hot-forming*. Steel Research International 80 (2009), 12, pp. 892-898

11. Nürnberger, F.; Grydin, O.; Schaper, M.; Bach, Fr.-W.; Koczurkiewicz, B.; Milenin, A.: *Microstructure transformations in tempering steels during continuous cooling from hot forging temperatures*. Steel Research 81 (2010), 3, pp. 224-233

12. Rios, P.R.: *Relationship between non-isothermal transformation curves and isothermal and non-isothermal kinetics*. Acta Materialia 53 (2005), 18, pp. 4893-4901

13. Bach, Fr.-W.; Schaper, M.; Yu, Z.; Nürnberger, F.; Gretzki, T.; Rodman, D.; Springer, R.: *Computation of isothermal transformation diagrams of 42CrMo4 steel from dilatometer measurements with continuous cooling*. International Heat Treatment and Surface Engineering 4 (2010), 4, pp. 171-175

14. Nürnberger, F.: *Vorhersage und Mikrostruktur und mechanischen Eigenschaften präzisionsgeschmiedeter Bauteile bei einer integrierten Wärmebehandlung*. Diss., Gottfried Wilhelm Leibniz Universität Hannover, 2010

15. Rakoski, F.: *Umformdilatometrie – Richtlinien zur Versuchsdurchführung*. Werkstoffprüfung 1991, 5.-6. Dec. 1991, Bad Nauheim, pp. 119-129

16. Hensel, A.; Spittel, T.: *Kraft- und Arbeitsbedarf bildsamer Formgebungsverfahren*. VEB Deutscher Verlag für Grundstoffindustrie, Leipzig 1978

Микроструктурные изменения в улучшаемых сталях в ходе горячей обработки давлением и закалки с температур деформации

Нюрнбергер Ф., Гридин А., Ю Ж., Шапер М.

Для разработки процесса точной объемной штамповки, совмещенного с термообработкой от нагрева при горячей штамповке, были построены при помощи деформационного дилатометра реологические кривые для старения и закалки различных сталей. Также были построены непрерывные диаграммы зависимости структурных превращений от температуры и времени для закалки и старения стали 42CrMo4. Эти диаграммы принимают во внимание влияние деформации на протекание превращений в ходе закалки от температуры 850 °C. Результаты исследований показывают увеличение напряжений пластического течения с уменьшением температуры и незначительное влияние деформации на конечную прочность материала и микроструктурные компоненты.